

The RHMC algorithm for theories with unknown spectral bounds.

J. B. Kogut*

Department of Energy, Division of High Energy Physics, Washington, DC 20585, USA

and

*Dept. of Physics – TQHN, Univ. of Maryland,
82 Regents Dr., College Park, MD 20742, USA*

D. K. Sinclair†

*HEP Division, Argonne National Laboratory,
9700 South Cass Avenue, Argonne, IL 60439, USA*

Abstract

The Rational Hybrid Monte Carlo (RHMC) algorithm extends the Hybrid Monte Carlo algorithm for lattice QCD simulations to situations involving fractional powers of the determinant of the quadratic Dirac operator. This avoids the updating increment (dt) dependence of observables which plagues the Hybrid Molecular-dynamics (HMD) method. The RHMC algorithm uses rational approximations to fractional powers of the quadratic Dirac operator. Such approximations are only available when positive upper and lower bounds to the operator's spectrum are known. We apply the RHMC algorithm to simulations of 2 theories for which a positive lower spectral bound is unknown: lattice QCD with staggered quarks at finite isospin chemical potential and lattice QCD with massless staggered quarks and chiral 4-fermion interactions (χ QCD). A choice of lower bound is made in each case, and the properties of the RHMC simulations these define are studied. Justification of our choices of lower bounds is made by comparing measurements with those from HMD simulations, and by comparing different choices of lower bounds.

*Supported in part by NSF grant NSF PHY03-04252.

†This work was supported by the U.S. Department of Energy, Division of High Energy Physics, Contract W-31-109-ENG-38.

I. INTRODUCTION

For lattice field theories with fermions, and in particular for lattice QCD, where there exists a local action describing the dynamics with the desired number of fermion flavours, the preferred simulation method is the hybrid Monte-Carlo (HMC) algorithm [1]. The HMC augments a hybrid molecular-dynamics update with a discrete ‘time’ step (dt), with a global accept/reject step at the end of each trajectory. This accept/reject step makes the algorithm exact, removing all dt dependence from measured observables.

For staggered and improved staggered fermions with numbers of flavours which are not multiples of 4 and for other fermion schemes with odd numbers of flavours, there is no local action, and one needs to take fractional powers of the fermion determinant. Until recently, simulations of such theories used hybrid molecular-dynamics simulations with ‘noisy’ fermions, usually the R algorithm (HMD(R)) [2]. The problem is that in HMD(R) simulations, the observables depend on dt , the leading departure from the desired $dt = 0$ results being $\mathcal{O}(dt^2)$. Hence one should either simulate at several (small) dt values and extrapolate to $dt = 0$, or perform simulations at such a small dt value that the $\mathcal{O}(dt^2)$ errors are negligible.

In the RHMC algorithm [3, 4, 5, 6, 7], instead of taking fractional powers of the determinant of the quadratic Dirac operator, one takes fractional powers of the operator itself. This defines an action (nonlocal) and thus permits a global accept/reject step. Since the quadratic Dirac operator is positive definite, such fractional powers are well defined in terms of the eigenmodes of the operator. To make this algorithm practical, one needs approximations to the fractional powers of the eigenvalues, which can be applied directly to matrices. The RHMC algorithm uses rational approximations and their partial-fraction expansions to approximate such fractional powers over the range of eigenvalues of the quadratic Dirac operator. Provided that the condition number (ratio of maximum to minimum eigenvalues) of this operator is not too large, sufficiently good approximations to this fractional power can be obtained with a modest order of numerator and denominator polynomials in this approximation.

The first theory we consider is lattice QCD at finite isospin chemical potential μ_I , but with no explicit symmetry breaking parameter [8, 9, 10]. The spectrum of the quadratic Dirac operator for this theory has an unknown lower bound. However, we can make a reasonable

guess as to what is a conservative estimate of the lower bound for the small μ_I values of interest. The need for such an exact algorithm is indicated, since, in HMD(R) simulations, the Binder cumulants which are used to determine the nature of the finite temperature phase transition for this theory depend strongly on dt [9, 10, 11, 12]. We have adapted the RHMC algorithm to this theory with 3-fermion flavours and tested the reversibility needed for its implementation. To check the validity of our speculative lower bound to the Dirac spectrum, we have compared our measurements with extrapolations to zero dt of our results from earlier HMD(R) simulations at various dt s. In addition, we have performed simulations using rational approximations which assume much smaller lower bounds to the spectrum, at the largest μ_I value and selected β and m values which we used with the original choice of bounds. Indications are that our original choice of lower bounds are adequate.

The second theory we are considering is 2-flavour lattice QCD at zero quark mass, using the χ QCD action, which incorporates an irrelevant chiral 4-fermion interaction that allows simulations at zero quark mass [13, 14]. Here again, we have reasonable estimates of the upper bound of the spectrum of the quadratic Dirac operator, but the lower bound is unknown. Again we make an educated guess as to what is a reasonably conservative lower bound for the spectrum of this operator and test our choice. For a $24^3 \times 8$ lattice, we found that using 32-bit floating point precision, was the main limit on reversibility. With 64-bit precision, the convergence criteria for the multimass Dirac operator inversion was the limiting factor, leading us to prefer using 64-bit precision. We tried 3 different choices of speculative lower bounds on the quadratic Dirac operator comparing the inversions at the beginning and at the end of each trajectory. For the 2 lowest choices, these inverses agreed to within the known accuracy of the rational approximations used, for all trajectories in the run. The highest choice agreed with the other 2 for almost all trajectories in the run. In addition we made direct comparison of the results of simulations using the RHMC algorithm with earlier measurements using the HMD(R) algorithm on small ($8^3 \times 4$) lattices.

Section 2 introduces the 2 theories under consideration with rational approximations. In section 3 we discuss the case of QCD at finite μ_I , while in section 4 we consider χ QCD. Finally in section 5 we present discussions and conclusions.

II. QCD AT FINITE μ_I , χ QCD AND RATIONAL APPROXIMATIONS

In this section we present two Lattice QCD actions for which the lower bound on the spectrum of the quadratic Dirac operator is unknown. This is important for the application of the RHMC algorithm for numbers of fermion flavours other than multiples of 8. One can only find a rational approximation to a fractional power α of a positive (semi-)definite matrix to any desired relative accuracy, if one knows positive lower and upper bounds to its spectrum.

If M is a positive (semi-)definite matrix with eigenvectors $|\lambda\rangle$ and corresponding (non-negative) eigenvalues λ , and α is a real number,

$$M^\alpha = \sum_{\lambda} \lambda^\alpha |\lambda\rangle\langle\lambda| \quad (1)$$

gives a unique definition of any real power of M . If one knows the spectral bounds on M i.e. that $0 < a \leq \lambda \leq b$, for some a and b , then one can find a rational approximation to λ^α of the form

$$\lambda^\alpha \approx P(\lambda)/Q(\lambda) \quad (2)$$

where P and Q are polynomials in λ , such that for a any given (small) positive ϵ

$$\text{Max}_{\lambda \in [a, b]} \frac{|\lambda^\alpha - P(\lambda)/Q(\lambda)|}{|\lambda^\alpha|} \leq \epsilon. \quad (3)$$

As $\epsilon \rightarrow 0$ or $a/b \rightarrow 0$, the orders of P and/or Q needed $\rightarrow \infty$. The method of calculating the best approximation for fixed orders of P and Q was specified by Remez. We use an implementation provided by Clark and Kennedy [15] (Note that this approximation also yields the best rational approximation to $\lambda^{-\alpha}$). This rational approximation to the eigenvalues of M^α provides a rational approximation to M^α itself as

$$M^\alpha \approx P(M)Q^{-1}(M), \quad (4)$$

which can be implemented directly in terms of the matrix M without having to find its eigenvalues and eigenvectors. Expanding the right-hand-side of equation 4 in terms of partial fractions allows the action of M^α on any vector to be calculated using a multishift conjugate gradient algorithm [16, 17] for little more than the cost of a single conjugate gradient inversion.

A. QCD at finite μ_I

Lattice QCD at finite isospin chemical potential μ_I , has the staggered quark action [8]

$$S_f = \sum_{\text{sites}} \left[\bar{\chi} \left[\mathcal{D} \left(\frac{1}{2} \tau_3 \mu_I \right) + m \right] \chi + i \lambda \epsilon \bar{\chi} \tau_2 \chi \right], \quad (5)$$

where $\mathcal{D}(\frac{1}{2}\tau_3\mu_I)$ is the standard staggered quark transcription of \mathcal{D} with the links in the $+t$ direction multiplied by $\exp(\frac{1}{2}\tau_3\mu_I)$ and those in the $-t$ direction multiplied by $\exp(-\frac{1}{2}\tau_3\mu_I)$. For finite temperature simulations with $\mu_I < m_\pi$, we set the coefficient λ of the explicit symmetry breaking term to zero. As it stands, this action describes 4 quark flavours (in the continuum limit).

To tune this to N_f flavours following the RHMC approach, we replace this with the pseudo-fermion action

$$S_{pf} = p_\psi^\dagger \mathcal{M}^{-N_f/8} p_\psi \quad (6)$$

where p_ψ is the momentum conjugate to the pseudo-fermion field ψ .

$$\mathcal{M} = \left[\mathcal{D} \left(\frac{1}{2} \tau_3 \mu_I \right) + m \right]^\dagger \left[\mathcal{D} \left(\frac{1}{2} \tau_3 \mu_I \right) + m \right] + \lambda^2 \quad (7)$$

is the quadratic Dirac operator, and we set $\lambda = 0$. To apply the RHMC algorithm we will need rational approximations to $\mathcal{M}^{-N_f/8}$ and $\mathcal{M}^{\pm N_f/16}$.

It is easy to see that $[\cosh(\frac{1}{2}\mu_I) + 3 + m]^2$ is an upper bound to the spectrum of \mathcal{M} . We, in fact, choose an upper bound of 25 which exceeds this bound for any choice of μ_I and m we are ever likely to consider. At $\mu_I = 0$, m^2 is a lower bound on the spectrum. One might expect that this bound is overly conservative, and that the actual lower bound would be closer to $\frac{1}{2}m_\pi$. For $\mu_I > 0$, we do not know the lower bound of the spectrum of the quadratic Dirac operator. However, the effective pion mass is $m_\pi - \mu_I$, so if this gives at least some guide as to the lower bound of this operator, we would expect the lower bound of its spectrum to decrease smoothly as μ_I is increased, becoming zero at $\mu_I = m_\pi$, the value of μ_I at the zero temperature transition to the superfluid phase. Our observations from HMD(R) simulations, indicate that in this low μ_I regime the Dirac operator becomes more singular as μ_I is increased, in a controlled way. Since we are interested in quark masses $m \geq 0.02$, we choose a speculative lower bound of 1.0×10^{-4} , 4 times lower than the known lower bound at $\mu_I = 0$ for $m = 0.02$. Tests are applied to see that this is reasonable. We restrict ourselves to the case $N_f = 3$.

B. χ QCD

The χ QCD staggered lattice action incorporates an irrelevant chiral 4-fermion interaction of the Gross-Neveu form, which allows us to run at zero quark mass. In terms of pseudo-fermion fields ψ and their conjugate momenta p_ψ the fermion action, modified for implementation of the RHMC algorithm is

$$S_{pf} = p_\psi^\dagger (A^\dagger A)^{-N_f/8} p_\psi \quad (8)$$

where

$$A = \mathcal{D} + m + \frac{1}{16} \sum_i (\sigma_i + i\epsilon\pi_i) \quad (9)$$

with i running over the 16 sites on the dual lattice neighbouring the site on the normal lattice, $\epsilon = (-1)^{x+y+z+t}$ and \mathcal{D} is the usual gauge-covariant ‘‘d-slash’’ for the staggered quarks. σ and π are the auxiliary fields which implement the 4-fermion interactions. The action for these auxiliary fields is

$$S_{\sigma\pi} = \sum_{\bar{s}} \frac{1}{8} N_f \gamma (\sigma^2 + \pi^2), \quad (10)$$

where the sum is over the sites of the dual lattice. For more details of the rest of the action we refer the reader to our earlier work [13]. We did, however make one minor change, multiplying the (σ, π) ‘kinetic energy’ by γ , which acts as a large mass and slows down the dynamics of these chiral fields.

Although we do not know the upper bound of the spectrum of the Dirac operator, because of the interaction with the chiral field, we know from our HMD(R) simulations that $\langle \frac{1}{8} N_f \gamma (\sigma^2 + \pi^2) \rangle$ is just above 1. For $N_f = 2$ and $\gamma = 10$ the coefficient $\frac{1}{8} N_f \gamma = 2.5$. This plus the fact that the σ and π interacting with the fermion fields at a given point are averages over 16 points on the dual lattice, suggest that 1 is a conservative upper bound for the contribution of the chiral fields to the eigenvalues of the Dirac operator. We thus assume an upper bound of 25 for the spectrum of the quadratic Dirac operator. If this were violated, it would only affect modes close to the ultraviolet cutoff on the theory, which are of limited interest. We shall later present evidence that the magnitude of the chiral field which interacts with the fermion field at a point is bounded by 1.

More important is an accurate knowledge of the lower bound on the spectrum of the quadratic Dirac operator. Here we simply assume that the action of the chiral fields on the

spectrum is similar to giving the quarks a small mass. Our speculative lower bound is that for a regular staggered action with a quark mass 0.001, i.e. 1×10^{-6} , and we perform tests of this assumption.

III. TESTS OF THE RHMC FOR LATTICE QCD AT FINITE μ_I .

The RHMC algorithm for QCD at a finite chemical potential μ_I for isospin is implemented following Clark and Kennedy [18]. The rational approximations are obtained using the Michael Clark's Remez code [15]. We have been using this method for simulating $N_f = 3$ flavour QCD. Here we use a (20, 20) rational approximation to $\mathcal{M}^{(3/16)}$ needed at the beginning of each trajectory, and a (20, 20) rational approximation to $\mathcal{M}^{(-3/16)}$ needed at the end of the trajectory to calculate the final 'energy' (value of the classical molecular-dynamics Hamiltonian describing the system), over the interval $[1 \times 10^{-4}, 25]$ discussed in section 2. These approximations have a maximum relative error of 6.1×10^{-12} . The evolution of the fields over the trajectories were performed using a (10, 10) rational approximation to $\mathcal{M}^{(-3/8)}$ over the interval $[1 \times 10^{-4}, 25]$, which has maximum relative error of 4.4×10^{-6} . Since we have been using relatively small lattices $8^3 \times 4$ and $12^3 \times 4$, we have found 32-bit floating-point precision (accumulations are performed in 64-bit precision) to be adequate.

For the RHMC algorithm to be exact, i.e. for it to produce an ensemble of configurations which have the correct Boltzmann distribution for the given action with no dt dependence, the updating algorithm must be reversible. The updating method specified by Kennedy et al. is reversible for infinite precision arithmetic, even when the multimass conjugate gradient solver used to invert the Dirac operator is stopped prior to convergence. (The inversions at the beginning and end of each trajectory still need to be exact for this to hold). With the finite precision used by computers, this reversibility must be tested. As mentioned above, we use single precision (32-bit) floating point arithmetic for simulations of lattice QCD at finite μ_I . To test this we performed a 1000 trajectory run on a $12^3 \times 4$ lattice at $\beta = 5.1285$, $m = 0.03$ and $\mu_I = 0.3$, in which every second trajectory was run forward and then reversed, returning to its initial state. $dt = 0.05$ for this experiment, and the trajectory length $\Delta t = 1$. $\mu_I = 0.3$ is chosen, because it is the largest μ_I used in our production runs. $m = 0.03$, just above the critical mass, is the smallest mass for which we run at $\mu_I = 0.3$, and $\beta = 5.1285$, close to the transition β for these values of m and μ_I , is one we use for production runs.

We expect therefore that the Dirac operator will be as close to singular as we will encounter in any of our simulations, and that if the algorithm is satisfactory here, it will work for the whole range of parameters we use.

The change in ‘energy’ δE , for each of the 500 reversed trajectories is plotted in figure 1a. The change in energy for each of the non-reversed trajectories is shown in figure 1b. We choose E as a measure of reversibility because it is the quantity that is used in the global Metropolis accept reject step. Hence departures of δE from zero, its value for true reversibility, indicate the size of errors introduced from departures from exact reversibility coming from finite precision errors potentially magnified by instabilities. As we see, these are indeed small in magnitude – $< 3 \times 10^{-3}$, and 3 orders of magnitude smaller than the change ΔE in energy over a typical trajectory used for normal updating. In addition, the average δE over the 500 trajectories considered is only $\approx 1.8 \times 10^{-4}$, indicating that there is no sign of a systematic bias, so that the small errors introduced by this lack of reversibility are likely to cancel.

Most of the simulations of lattice QCD at finite isospin density, which we have run using this code use $dt = 0.05$, and all use trajectory length $\Delta t = 1$. With this choice we find an acceptance rate of $\sim 70\%$ for the generated trajectories. Most of our runs used the same β for the updating as for the global Metropolis step, since we did not find large gains from choosing different β s.

We check our speculative lower bound on the spectrum of the quadratic Dirac operator of 1×10^{-4} , at our largest μ_I ($\mu_I = 0.3$) at both masses (0.03 and 0.035) where we performed production simulations. This we did by running using rational approximations, valid over intervals with the same upper bound, but different lower bounds, and compared observables. At $m = 0.035$, $\mu_I = 0.3$ and $\beta = 5.1370$, we performed a 300,000 trajectory run with rational approximations valid over the interval $[1 \times 10^{-4}, 25]$ used for production running and a 300,000 trajectory run with the same rational approximation for updating, but a (20, 20) rational approximation valid over the range $[1 \times 10^{-5}, 25]$ for initiating each trajectory and for calculating the energy at the end of each trajectory. This approximation has maximum relative error of 2.0×10^{-10} . A comparison of the observables from these 2 simulations is given in table Ia. At $m = 0.03$, $\mu_I = 0.3$, $\beta = 5.1290$ we ran one 300,000 trajectory run with rational approximations valid over our default interval ($[1 \times 10^{-4}, 25]$) and one 300,000 trajectory run with rational approximations valid over the interval $[1 \times 10^{-6}, 25]$

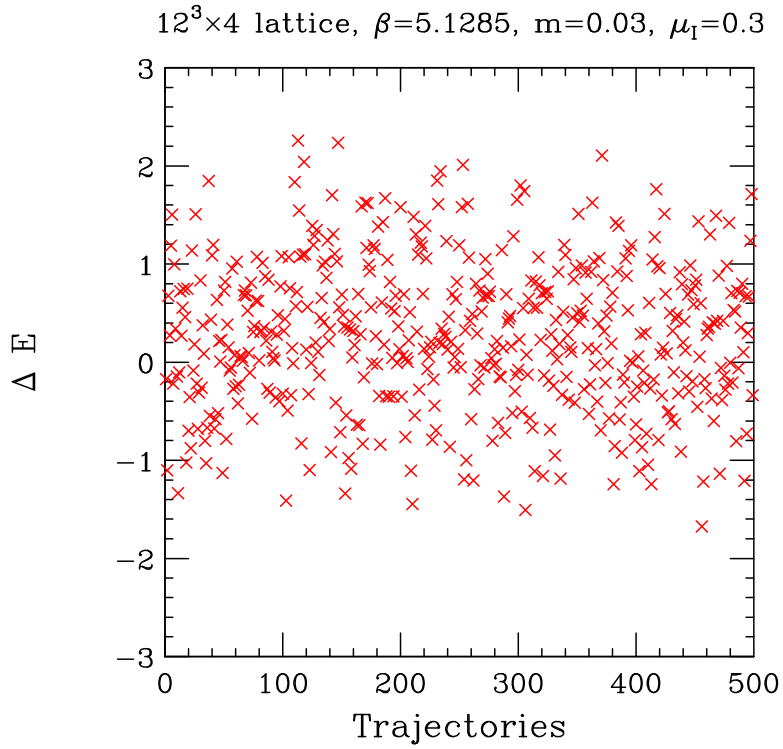
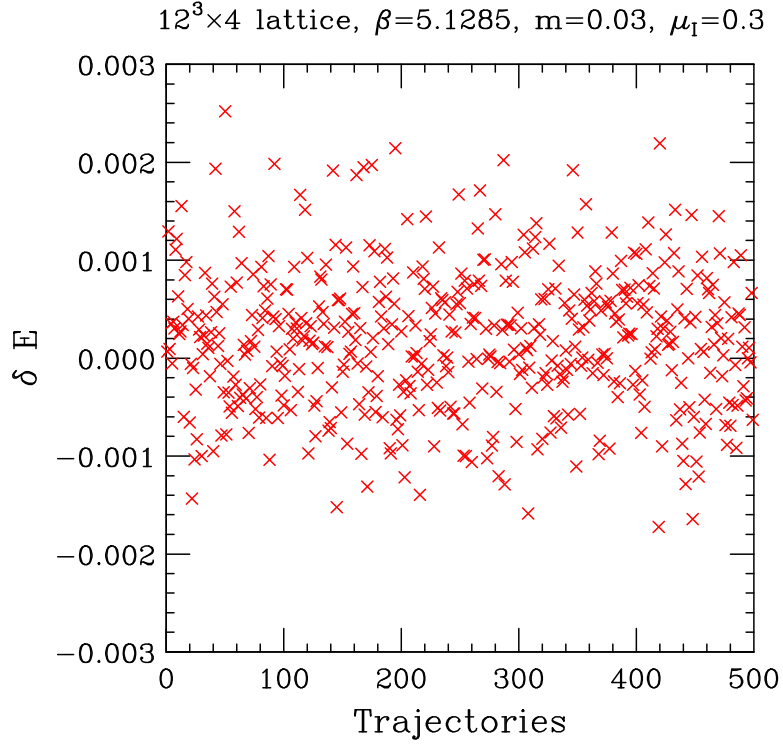


FIG. 1: a) The energy change for ‘closed’ trajectories ($t \rightarrow t + 1 \rightarrow t$). b) The energy change for ‘open’ ($t \rightarrow t + 1$) trajectories.

for initialization, measurement *and* updating each trajectory. For this later interval we used

(25, 25) rational approximations with maximum relative error 2.0×10^{-11} at the ends of each trajectory and (15, 15) rational approximations with a maximum relative error of 7.2×10^{-7} for the updating. Observables from these 2 runs are compared in table Ib.

$m = 0.035, \mu_I = 0.3, \beta = 5.1370$		
Spectrum range	$[1 \times 10^{-4}, 25]$	$[1 \times 10^{-5}, 25]$
B_4	1.860(36)	1.879(41)
β_c	5.13744(24)	5.13787(22)
plaquette	0.51086(66)	0.51134(60)
Wilson Line	0.3300(74)	0.3245(68)
$\langle \bar{\psi}\psi \rangle$	0.6274(94)	0.6347(86)
j_0^3	0.0450(10)	0.0442(10)

$m = 0.03, \mu_I = 0.3, \beta = 5.1290$		
Spectrum range	$[1 \times 10^{-4}, 25]$	$[1 \times 10^{-6}, 25]$
B_4	1.704(30)	1.722(39)
β_c	5.12826(18)	5.12820(21)
plaquette	0.50776(60)	0.50753(68)
Wilson Line	0.3773(68)	0.3792(76)
$\langle \bar{\psi}\psi \rangle$	0.5442(80)	0.5411(103)
j_0^3	0.0529(10)	0.0532(11)

TABLE I: Comparison of observables measured during RHMC simulations with different speculative lower bounds for the spectrum of the quadratic Dirac operator: a) For $m = 0.035, \mu_I = 0.3, \beta = 5.1370$. b) For $m = 0.03, \mu_I = 0.3, \beta = 5.1290$.

The good agreement between the ‘data’ produced with the different values for the speculative lower bound indicates that our initial choice of 1×10^{-4} was adequate. One notes that, despite the high statistics – 300,000 trajectories for each run, the error bars are sizable. This is because the chosen β values are very close to β_c , the transition β , in each case which serves to maximize the fluctuations.

Finally we compare the values of two fluctuation quantities, the Binder cumulant $B_4(\bar{\psi}\psi)$ and the chiral susceptibility $\chi_{\bar{\psi}\psi}$ at β_c with results obtained from our HMD(R) simulations

over a range of dt values for $m = 0.035$ and an intermediate value of μ_I , $\mu_I = 0.2$, in figure 2. The leading errors in HMD(R) are expected to be $\mathcal{O}(dt^2)$. The fits linear in dt^2 in these figures appear to support this expectation, but indicate that we would need to include an $\mathcal{O}(dt^4)$ term to fit over the whole range of measurements. We note that the finite dt errors in both these graphs are quite large, so that agreement between HMD(R) and RHMC is non-trivial.

IV. TESTS OF RHMC FOR χ QCD

Since we have been simulating the thermodynamics of χ QCD with 2 massless quark flavours on $16^3 \times 8$ and $24^3 \times 8$ lattices, we use this larger lattice to run our tests. On this size lattice, extensive comparisons with the HMD(R) algorithm over a range of dt values is impractical, as is performing high statistics runs with various speculative lower bounds.

Our first tests used a single-precision (32-bit floating-point) version of the code, then a modified version where the multimass conjugate gradient inversions which initiate and end each trajectory were replaced with double-precision (64-bit floating-point) versions, while leaving the inversion routines which perform the updates within each trajectory in single precision. We then performed reversibility tests of the same nature as those described in the previous section. For the updating, our convergence criterion was applied to the normalized conjugate gradient residual for the lowest lying pole in the partial fraction expansion of the rational approximation, while at the beginning and end of each trajectory it was applied to the unnormalized residual. (If x_0 is an approximate solution to the linear equations $Ax = b$, the unnormalized residual is $r_u = |b - Ax_0|$. The normalized residual is $r_n = r_u/|b|$.) We denote this upper limit on these residuals by r and note that, since our sources are extensive, this means that we are using a much more stringent convergence criterion at the beginning and end of each trajectory than in the updating, as required.

Figure 3a shows the changes in energy over the ‘closed’ trajectories $t \rightarrow t + 1 \rightarrow t$ for the single precision code and for the same code with the initial and final inversions for each trajectory performed in double precision. $r = 0.001$ for these runs, since we have determined that no improvement is obtained by decreasing r below this value. $\beta = 5.535$, used for these simulations, is close to the critical point. The trajectory length is 1 time unit and $dt = 0.025$ which gives an acceptance of $\approx 75\%$. However, we turn off the accept/reject step in the

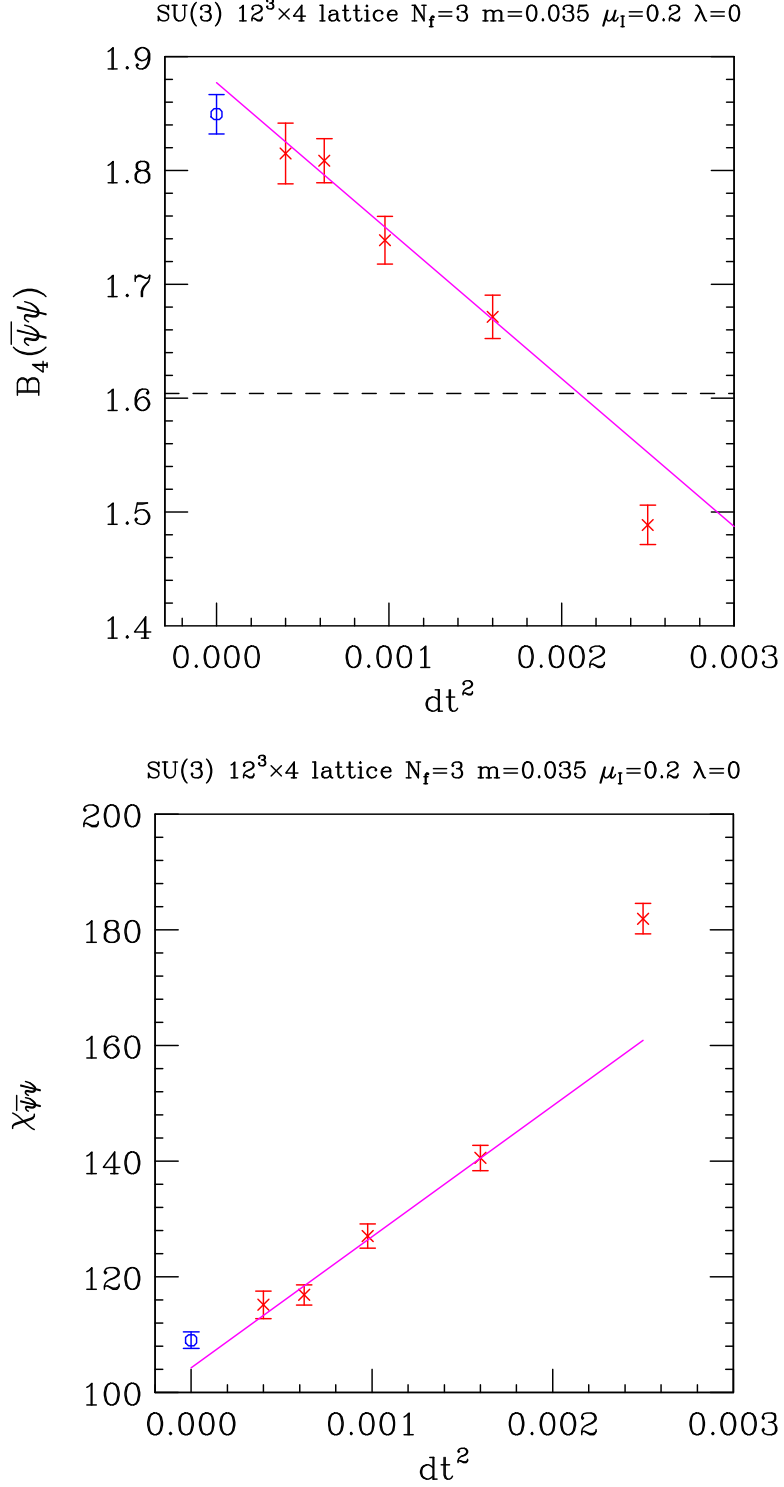


FIG. 2: a) The Binder cumulant $B_4(\bar{\psi}\psi)$ as a function of dt^2 for the HMD(R) algorithm (crosses) and the RHMC algorithm (circle at $dt = 0$). b) The chiral susceptibility $\chi_{\bar{\psi}\psi}$ as a function of dt^2 for the HMD(R) algorithm (crosses) and the RHMC algorithm (circle at $dt = 0$).

RHMC algorithm for the purpose of these reversibility tests to speed up the passage of the system through phase space. The single precision code produces energy changes as large as $\sim 6 \times 10^{-3}$. More troubling is the fact that δE is strongly biased to positive values. In fact the average δE is $\approx 2.6 \times 10^{-3}$ which suggests that this code could produce small but significant systematic errors. The mixed single/double precision code shows more promise and we have extended our run to include 500 closed trajectories as shown in figure 3b. The maximum value of $|\delta E|$ is $\approx 6.4 \times 10^{-3}$, which is larger than we would prefer. More problematic is that the average δE over the range is $\approx 1.1 \times 10^{-3}$, which suggests a systematic bias as is apparent in figure 3b. Unfortunately, we are limited by precision from improving this situation. We thus feel that to be safe we should increase the precision, especially if we wish to allow ourselves the option of increasing the lattice size in the future.

We have tested reversibility of our double precision code as a function of the residual r . The results for 50 closed trajectories are shown in figure 4. We see that this measure of reversibility of the trajectories improves considerably as r is decreased from 0.01 to 0.001. Comparing this graph with that for the single precision tests, we see that precision is indeed the limiting factor. Further tests indicate that it is the convergence of the approximate inversions during the updating (rather than that of the more precise inversions at the start and end of each trajectory) that is the limiting factor. Careful monitoring of the trajectories for the $r = 0.01$ run, indicates that this is largely due to the fact that the number of iterations of the conjugate gradient inverter sometimes differed by 1 or 2 iterations between the corresponding steps of the forward and reversed trajectories, and this of course has the largest effect when one is far from convergence. This can be corrected by running for a fixed number of conjugate gradient iterations rather than at fixed r . Since at $r = 0.01$ it requires around 250 iterations on average for the inversion at each update, we performed a run of 1000 trajectories with the number of inverter iterations at each update set to 300 (those at the ends of the trajectories were still set by a conservative choice of r). The results of running for 1000 trajectories (500 closed) with the number of conjugate gradient iterations fixed at 300 are shown in figure 5a along with an identical number of trajectories with these inversions set by $r = 0.002$. The maximum value of $|\delta E|$ for the case where the number of conjugate gradient iterations is fixed at 300 is $\sim 5 \times 10^{-3}$, no better than the single precision results. For $r = 0.002$ the maximum value of $|\delta E|$ is $\sim 1.5 \times 10^{-3}$ which we consider acceptable. The reason that fixing the number of conjugate gradient iterations at a relatively small value

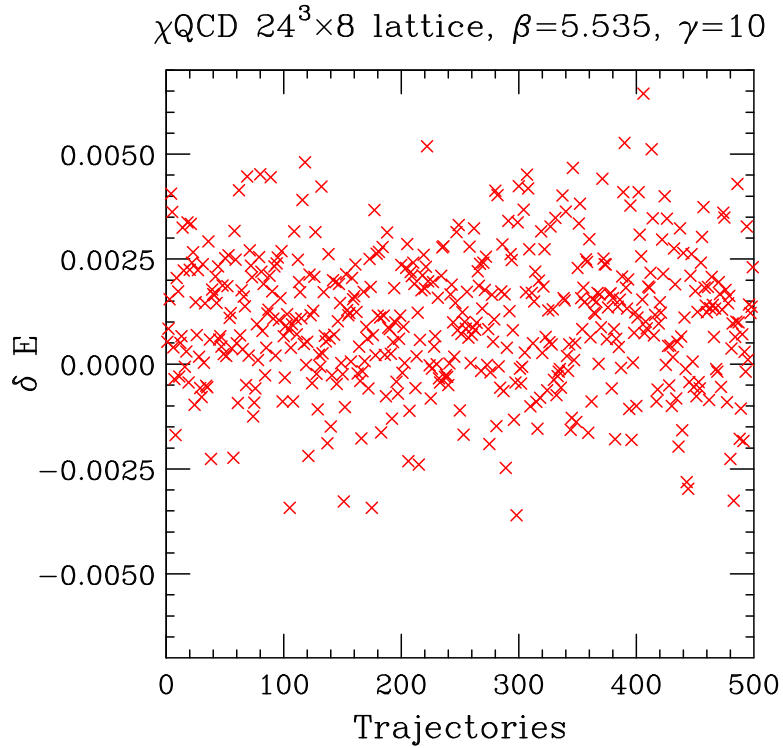
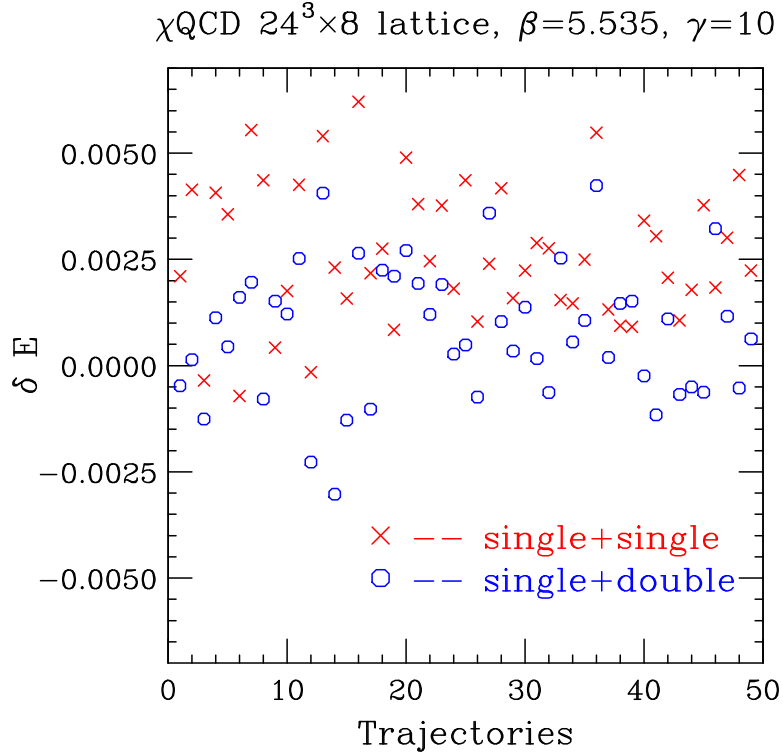


FIG. 3: a) Change in energy δE for 50 closed trajectories for single precision code (single-single) and single precision updating with double precision initialization and measurement for each trajectory (single-double). b) 500 closed trajectories for single-double code.

χ QCD $24^3 \times 8$ lattice, $\beta=5.535$, $\gamma=10$

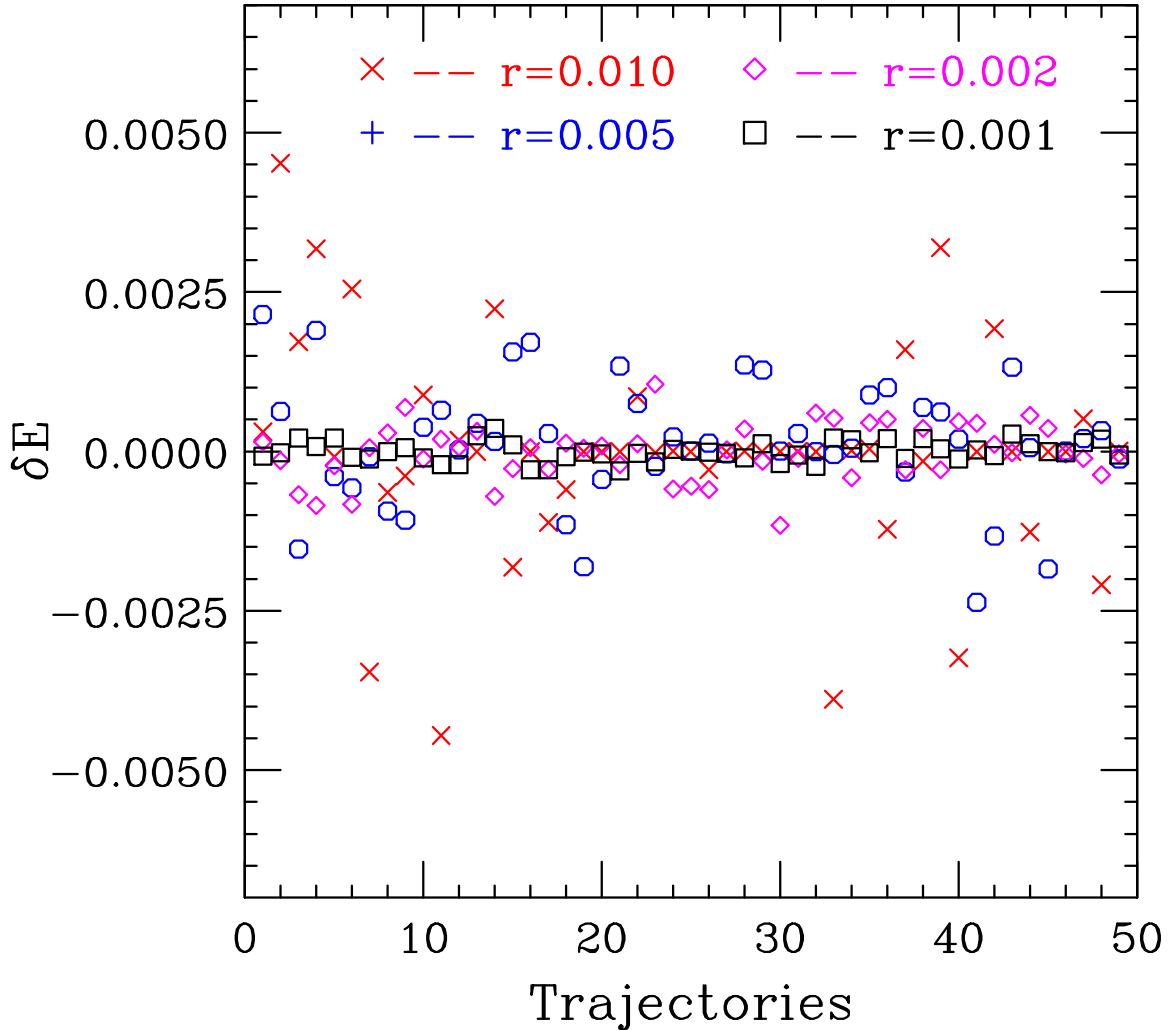


FIG. 4: The change in energy δE for closed trajectories for a range of choices of r for 64-bit precision code.

did not give better results is presumably because this gives relatively poor convergence for some configurations. Studies of the HMC algorithm have indicated that if the convergence is too poor, the updating procedure develops instabilities which amplify the effects of finite precision errors [19]. We believe that such instabilities are most likely the reason why using a fixed number of conjugate gradient iterations during updating did not lead to smaller violations of reversibility. Figure 5b shows the change of energies for the open trajectories from the same $r = 0.002$ run.

We now need to justify our choices of spectral bounds on the quadratic Dirac operator.

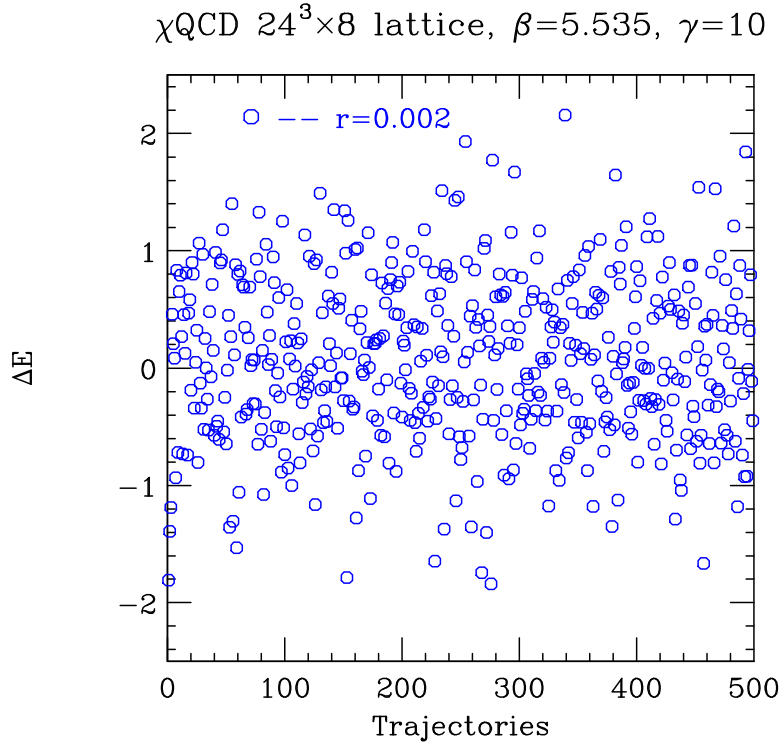
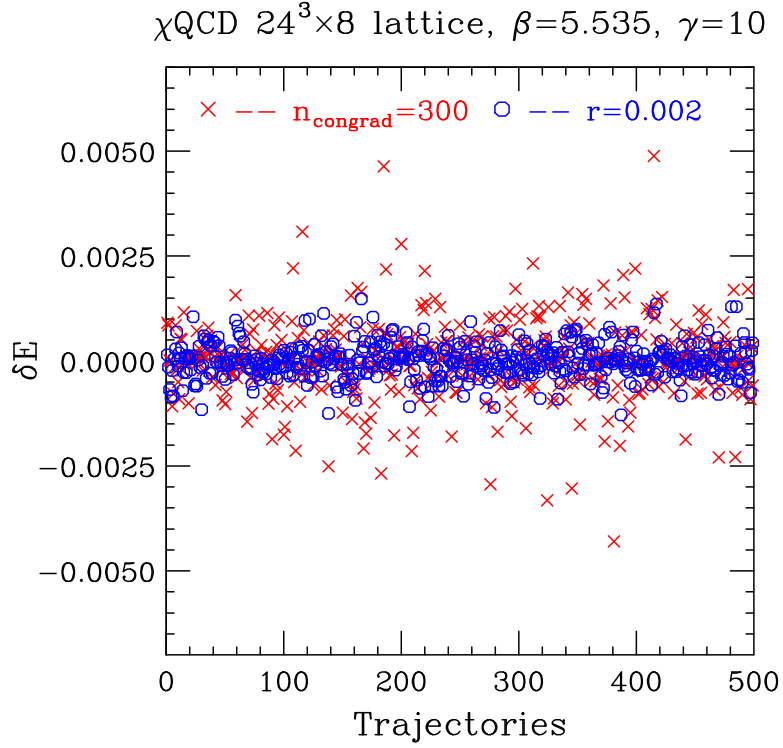


FIG. 5: a) The change in energy δE for closed trajectories for a fixed number of conjugate gradient iterations and for $r = 0.002$. b) The change in energy ΔE for open trajectories for $r = 0.002$.

The chosen upper bound of 25 is obtained assuming that the magnitude of the average of

the 16 chiral auxiliary fields $\sigma + i\pi$ which couple to the fermion bilinear $\bar{\psi}\psi$ at each site is bounded above by 1. Figure 6 shows the maximum over the lattice sites of the magnitude of $\sigma + i\pi$ at the beginning and end of 3000 trajectories of our production running at $m = 0$, $\beta = 5.535$, $\gamma = 10$, $dt = 0.03125$, trajectory length 1 and $r = 0.002$, where the acceptance is around 60–70%. As can be seen, 1 is a conservative upper bound for $|\sigma + i\pi|$.

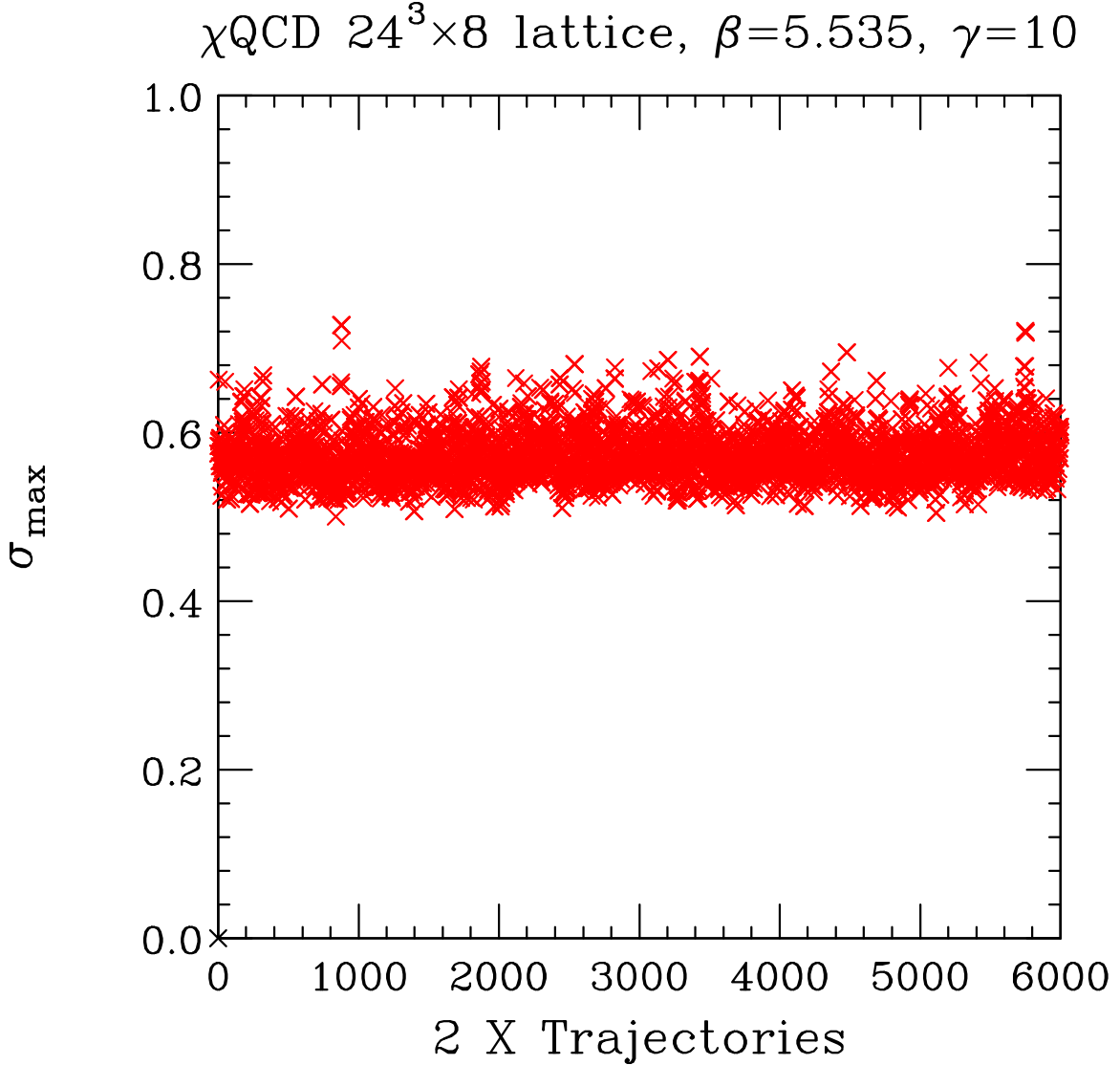


FIG. 6: Maximum values of $|\sigma + i\pi|$ at the start and end of each trajectory of a production run.

Since we are using a relatively large lattice ($24^3 \times 8$) it is not practical to obtain adequate statistics close to the phase transition with more than one choice of speculative lower bounds as was done with our simulations of lattice QCD at finite isospin chemical potential, in order to check for consistent results. Instead, we performed a simulation of 1000 trajectories with

a speculative lower bound of 1×10^{-8} . At the beginning of each trajectory where we calculate the momenta p_ψ conjugate to the pseudo-fermion fields, as

$$p_\psi = \mathcal{M}^{1/8}\xi, \quad (11)$$

we compared the values of p_ψ obtained with rational approximations which assume lower bounds of 1×10^{-6} , 1×10^{-8} and 1×10^{-10} . These used (25, 25), (30, 30), and (35, 35) rational approximations respectively, with maximum relative errors of 1.4×10^{-11} , 3.0×10^{-11} and 4.9×10^{-11} respectively. Similar comparisons were made of the ξ s at the end of each trajectory reconstituted as

$$\xi = \mathcal{M}^{-1/8}p_\psi. \quad (12)$$

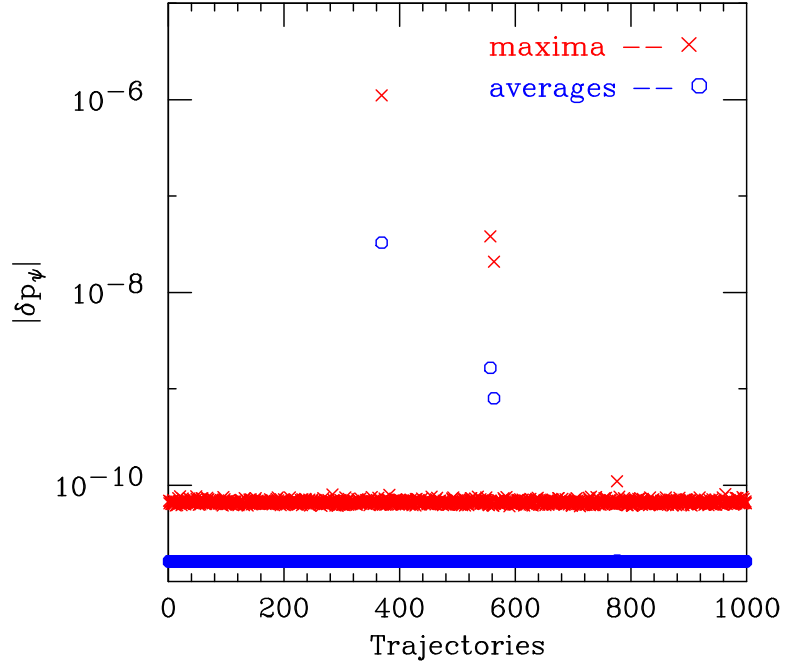
No comparisons with results from using different speculative lower bounds were made during the updates, since using different rational approximations corresponds to making different choices of the updating Hamiltonian, and such choices are unimportant unless they significantly affect the acceptance.

In figure 7a, we show the magnitude of the difference between p_ψ values calculated using a lower bound of 1×10^{-6} and those using a lower bound of 1×10^{-8} . We plot the maximum over sites and colours of this quantity for each trajectory as well as the average over sites and colours. Figure 7b shows such differences for ξ . For 997 of these trajectories, the differences in p_ψ , and ξ values are consistent with zero within the accuracies of the rational approximations we use. For the other 3 trajectories, the differences are much larger. In addition, we note that the configurations which give relatively large errors for p_ψ , and for ξ , are identical. Figure 8 shows differences between the same quantities for lower bounds of 10^{-8} and 10^{-10} respectively for the *same* trajectories as in figure 7. In this case all differences are consistent with zero within the accuracy of the rational approximations we use.

We interpret these results as indicating that for 997 of the configurations generated, all eigenvalues of the quadratic Dirac operator are $\gtrsim 10^{-6}$. For the remaining 3 configurations, the minimum eigenvalues lie between 10^{-8} and 10^{-6} . It is reassuring to note that even for these configurations the differences are small, since a typical p_ψ or χ has a magnitude $\mathcal{O}(1)$. Hence it is probably reasonable to use a speculative lower bound of 10^{-6} and, unless this run was anomalous, choosing a speculative lower bound of 10^{-8} is completely safe.

Finally we present some results from small lattice ($8^3 \times 4$) simulations using the RHMC algorithm for χ QCD and compare them with earlier published results using the HMD(R)

χ QCD $24^3 \times 8$ lattice, $\beta=5.535$, $\gamma=10$



χ QCD $24^3 \times 8$ lattice, $\beta=5.535$, $\gamma=10$

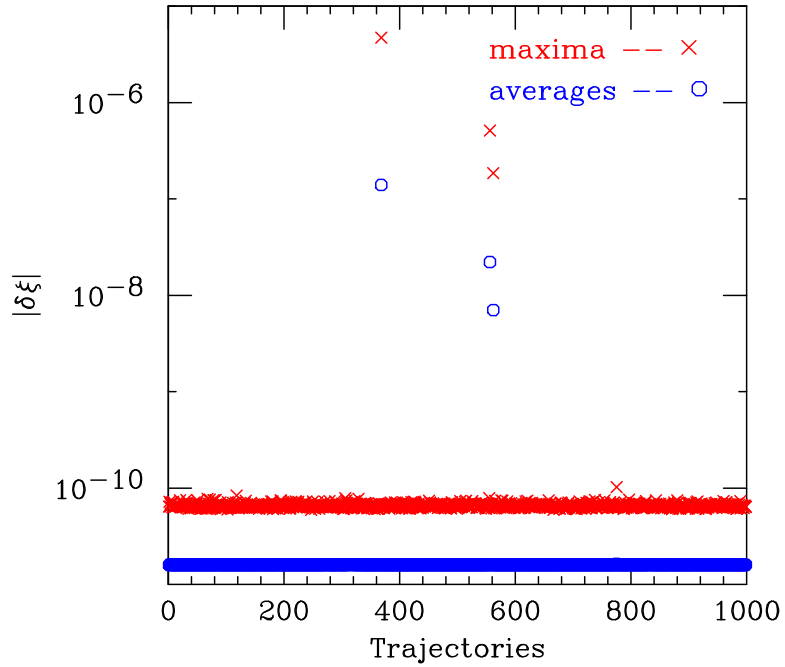
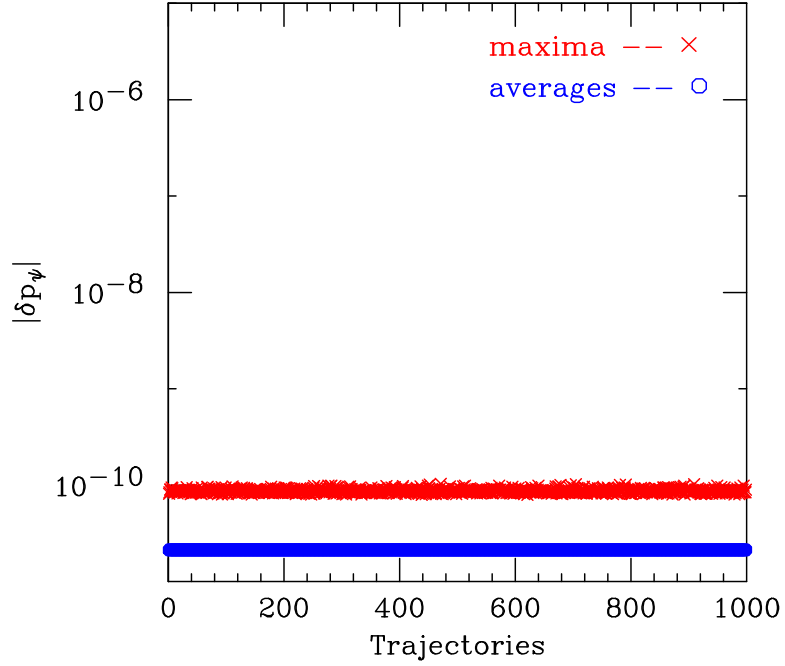


FIG. 7: a) Magnitude of the difference between p_ψ values using speculative lower bounds of 10^{-6} and 10^{-8} . b) Magnitude of the difference between ξ values using speculative lower bounds of 10^{-6} and 10^{-8} .

χ QCD $24^3 \times 8$ lattice, $\beta=5.535$, $\gamma=10$



χ QCD $24^3 \times 8$ lattice, $\beta=5.535$, $\gamma=10$

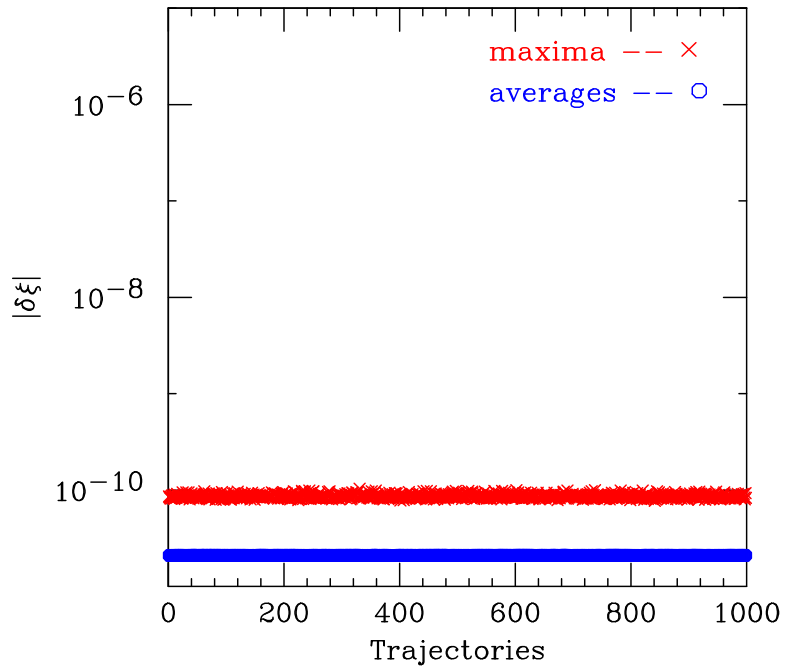


FIG. 8: a) Magnitude of the difference between p_ψ values using speculative lower bounds of 10^{-10} and 10^{-8} . b) Magnitude of the difference between ξ values using speculative lower bounds of 10^{-10} and 10^{-8} .

algorithm [13]. For such small lattices precision is not an issue and these simulations were performed using 32-bit floating-point arithmetic. Table IIa gives the results for $\gamma = 10$, $m = 0$ for our RHMC simulations over a range of β values which bracket the phase transition. We ran 100,000 trajectories for each β . Table IIb gives the published results for the same parameters for the HMD(R) algorithm. Considering the relatively low statistics of the earlier

β	Wilson Line	$\langle\bar{\psi}\psi\rangle$	$\langle\sigma\rangle$	Plaquette
5.0	0.0253(3)	1.2192(4)	0.1227(2)	0.58256(5)
5.1	0.0300(4)	1.1556(6)	0.1167(3)	0.56450(7)
5.2	0.0397(5)	1.0620(8)	0.1071(3)	0.54258(8)
5.3	0.0832(17)	0.9008(20)	0.0916(4)	0.51422(16)
5.4	0.6006(12)	0.1328(19)	0.0205(3)	0.46210(6)
5.5	0.6838(8)	0.0946(13)	0.0178(3)	0.44672(5)

TABLE II: a) Observables measured in RHMC simulations on an $8^3 \times 4$ with $\gamma = 10$, $m = 0$.

β	Wilson Line	$\langle\bar{\psi}\psi\rangle$	$\langle\sigma\rangle$	Plaquette
5.0	0.025(2)	1.217(3)	0.1235(5)	0.5825(3)
5.1	0.031(2)	1.147(2)	0.1170(5)	0.5636(3)
5.2	0.031(4)	1.065(4)	0.1080(5)	0.5430(8)
5.3	0.073(7)	0.910(5)	0.0923(8)	0.5149(7)
5.4	0.595(7)	0.131(5)	0.0203(8)	0.4619(4)
5.5	0.679(5)	0.093(3)	0.0173(6)	0.4469(3)

TABLE II: b) Observables measured in HMD(R) simulations on an $8^3 \times 4$ with $\gamma = 10$, $m = 0$.

HMD(R) results, the agreement with the RHMC simulations is excellent and the finite dt errors are small in this case.

V. DISCUSSIONS AND CONCLUSIONS

We have implemented the RHMC for 2 lattice actions where the lower bound on the spectrum of the quadratic Dirac operator is unknown. The first is the action for staggered lattice QCD with a finite chemical potential μ_I for isospin, in the small μ_I regime. The

second is the χ QCD action where the standard staggered quark action is augmented with a chiral 4-fermion interaction which allows simulations at zero quark mass. In the first case we simulate 3 fermion flavours, in the second 2. Both situations require taking a fractional power of the fermion determinant so that standard HMC methods fail, and the alternative HMD(R) algorithm gives finite dt errors. In each case the RHMC algorithm is implemented using a speculative lower bound to this spectrum, and its validity is tested by simulations. This rather naive approach appears successful in both cases.

In each case we test the reversibility of our implementation. This would be exact for infinite precision arithmetic and exact inversions at the beginning and ending of the trajectories. We test this by reversing our trajectories and determining how close we come to the initial state. The measure of this is the difference between the classical energy of this final configuration and that of the initial configuration. Since energy differences appear in the global Metropolis accept/reject step at the end of each trajectory, this energy difference should be much less than one. Because this energy is an extensive quantity, this requirement becomes more stringent as the lattice size is increased. For QCD at finite μ_I , we are using $12^3 \times 4$ lattices for which we find single-precision (32-bit) floating-point arithmetic to be adequate. For χ QCD, where we are simulating on $24^3 \times 8$ lattices double-precision arithmetic appears desirable. Here we have also studied convergence requirements on the inversions needed to implement the rational approximations, both at the beginning and end of the trajectory and in the updating. Those at the beginning and end of each trajectory need to be performed with high precision. The inversions in the updating can be performed with less precision. If these updating inversions are too imprecise, the change in energy will be large and the final configuration will not be accepted. It appears, however, that the instabilities due to finite precision are worse when these inversions are too imprecise, and this is more important in determining the minimum acceptable precision than are acceptance criteria.

For QCD at finite μ_I we test our speculative lower spectral bounds by 2 methods. First we find that the RHMC results for Binder cumulants and chiral susceptibilities agree with extrapolations of our HMD(R) results to $dt = 0$, and that the position of the transitions calculated from both types of simulation appear consistent. Second, at the largest μ_I we use, we check that all observables and fluctuation quantities at the transition agree with those obtained with simulations using speculative lower bounds which are 10 or 100 times smaller than our initial choice. This indicates that a lower bound of 10^{-4} is adequate.

For χ QCD, we find good agreement between measurements made using RHMC simulations and those made using HMD(R) simulations on $8^3 \times 4$ lattices. With our production lattice sizes of $24^3 \times 8$, it is impractical to make such detailed comparisons between the 2 methods. In addition making runs with sufficient statistics to compare different speculative lower bounds is also too expensive. Instead, we have compared applying rational approximations which assume different lower bounds to a set of 1000 configurations generated during one of our runs. We find agreement to within the accuracy of our rational approximations for speculative lower bounds of 10^{-8} and 10^{-10} . An approximation using a speculative lower bound of 10^{-6} agrees with that using a speculative lower bound of 10^{-8} on most of these configurations. Even in those cases where the two estimates do not agree, the differences are small enough that the errors introduced in a production run would probably be negligible. We conclude therefore that a lower bound of 10^{-8} is almost certainly acceptable, and one of 10^{-6} is probably acceptable. We did apply this test to our QCD at finite μ_I simulations comparing speculative lower bounds of 10^{-4} and 10^{-6} . Although there is no indication of any difference within the precision of our measurements, the limitation of 32-bit precision prevents us from using this test to make definitive statements.

We conclude that the use of speculative lower bounds for the spectrum of the quadratic Dirac operator is adequate to allow use of the RHMC exact algorithm to simulate either of the theories we have considered. For theories where it is necessary to determine the lower bound dynamically, comparisons between the results of different speculative lower bounds could be made from a set of choices starting with that with the largest lower bound, during a run (as we have done), and choosing the first approximation which passes the test. This way the expensive calculations of the rational approximations using the Remez method, need only be performed once. The order of the rational approximation required to achieve the desired accuracy with a given lower bound does not increase very rapidly as that bound is increased. For example, in our applications where the relative error is always less than 5×10^{-11} , we achieve this for the 2-flavour case using a (20, 20) rational approximation for a lower bound of 10^{-4} , a (25, 25) approximation for 10^{-6} , a (30, 30) approximation for 10^{-8} , and a (35, 35) approximation for 10^{-10} . Hence the ‘library’ of rational approximations one would need to maintain for such an implementation would be rather small. Such methods could be useful for domain-wall fermions and overlap fermions which have the problem that their lower spectral bounds are also unknown, and might need to be determined dynamically

[18].

Acknowledgements

We thank Philippe de Forcrand and Owe Philipsen for helpful discussions. The computations we have reported were performed on Bassi and Jacquard at NERSC, Tungsten and Cobalt at NCSA, DataStar at NPACI/SDSC and Jazz at the LCRC at Argonne National Laboratory. Access to the NSF computers was through an NRAC allocation.

-
- [1] S. Duane, A. D. Kennedy, B. J. Pendleton and D. Roweth, *Phys. Lett. B* **195**, 216 (1987).
 - [2] S. A. Gottlieb, W. Liu, D. Toussaint, R. L. Renken and R. L. Sugar, *Phys. Rev. D* **35**, 2531 (1987).
 - [3] A. D. Kennedy, I. Horvath and S. Sint, *Nucl. Phys. Proc. Suppl.* **73**, 834 (1999) [arXiv:hep-lat/9809092].
 - [4] M. A. Clark and A. D. Kennedy, *Nucl. Phys. Proc. Suppl.* **129**, 850 (2004) [arXiv:hep-lat/0309084].
 - [5] M. A. Clark, A. D. Kennedy and Z. Sroczynski, *Nucl. Phys. Proc. Suppl.* **140**, 835 (2005) [arXiv:hep-lat/0409133].
 - [6] M. A. Clark, P. de Forcrand and A. D. Kennedy, *PoS LAT2005*, 115 (2006) [arXiv:hep-lat/0510004].
 - [7] M. A. Clark, plenary talk presented at Lattice2006, Tucson (2006).
 - [8] J. B. Kogut and D. K. Sinclair, *Phys. Rev. D* **70**, 094501 (2004) [arXiv:hep-lat/0407027].
 - [9] J. B. Kogut and D. K. Sinclair, parallel talk presented at Lattice2006, Tucson (2006).
 - [10] J. B. Kogut and D. K. Sinclair, arXiv:hep-lat/0509095.
 - [11] O. Philipsen, *PoS LAT2005*, 016 (2006) [*PoS JHW2005*, 012 (2006)] [arXiv:hep-lat/0510077].
 - [12] P. de Forcrand and O. Philipsen, arXiv:hep-lat/0607017.
 - [13] J. B. Kogut, J. F. Lagae and D. K. Sinclair, *Phys. Rev. D* **58**, 034504 (1998) [arXiv:hep-lat/9801019].
 - [14] J. B. Kogut and D. K. Sinclair, *Phys. Rev. D* **73**, 074512 (2006) [arXiv:hep-lat/0603021].

- [15] M.A. Clark and A.D. Kennedy, <http://www.ph.ed.ac.uk/~mike/remez> (2005).
- [16] A. Frommer, B. Nockel, S. Gusken, T. Lippert and K. Schilling, *Int. J. Mod. Phys. C* **6**, 627 (1995) [arXiv:hep-lat/9504020].
- [17] B. Jegerlehner, arXiv:hep-lat/9612014.
- [18] M.A. Clark, talk presented at "Modern Challenges for Lattice Field Theory", Kavli Institute for Theoretical Physics, University of California, Santa Barbara (2005).
- [19] B. Joo, B. Pendleton, A. D. Kennedy, A. C. Irving, J. C. Sexton, S. M. Pickles and S. P. Booth [UKQCD Collaboration], *Phys. Rev. D* **62**, 114501 (2000) [arXiv:hep-lat/0005023].